Passive Seismic Characterization of High Priority Salt Jugs (15B, 59, 7A, 4A, 2A) Hutchinson, Kansas: August 2020

Sarah L. Morton, Erik Knippel, Shelby L. Peterie, Julian Ivanov, Richard D. Miller, Joe Anderson, Brett C. Bennett, Cole Bunker, Connor Umbrell, and Brett Wedel

Kansas Geological Survey
1930 Constant Avenue
Lawrence, KS 66047

Report to

Narayanan Raghupathi
Burns & McDonnell Engineering Company Inc.
1431 Opus Place, Suite 400
Downers Grove, IL 60615
630-724-3259

Open-file Report 2021-9 October 2020

The Kansas Geological Survey makes no warranty or representation, either express or implied, with regard to the data, documentation, or interpretations or decisions based on the use of this data including the quality, performance, merchantability, or fitness for a particular purpose. Under no circumstances shall the Kansas Geological Survey be liable for damages of any kind, including direct, indirect, special, incidental, punitive, or consequential damages in connection with or arising out of the existence, furnishing, failure to furnish, or use of or inability to use any of the database or documentation whether as a result of contract, negligence, strict liability, or otherwise. This study was conducted in complete compliance with ASTM Guide D7128-05. All data, interpretations, and opinions expressed or implied in this report and associated study are reasonably accurate and in accordance with generally accepted scientific standards.

Passive Seismic Characterization of High Priority Salt Jugs (15B, 59, 7A, 4A, 2A) Hutchinson, Kansas: August 2020

Executive Summary

This project appraised time-lapse stress conditions of rock above selected (15B, 59, 7A, 4A, 2A) dissolution voids by estimating the relative stress field from the calculated shear-wave velocity of the overburden. Shear-wave velocities were calculated using passive surface-wave methods. Data were acquired along five profiles located on or near key abandoned brine production wells using train traffic as an energy source. Multichannel analysis of surface waves (MASW) method was used to estimate the shear-wave velocity, at a resolution sufficient to loosely map the alluvial/bedrock contact and velocity characteristics of the Permian-aged Shale above the top of the "three finger" dolomite (at approximately 100 meters below ground surface). A key outcome was the differentiation of the rock properties based on their shear velocity above salt jugs (associated with the target wells) compared to rocks above undisturbed salt or jugs without roof rock under stress. Comparisons of shear-wave velocity profiles over time (time lapse) provided insights into overburden stability and therefore indirectly, void dynamics.

Passive MASW data were continuously acquired above five high priority wells over one night (August 20-21, 2020) on the Vigindustries site in Hutchinson, Kansas. A continuous sampling approach was used to record all available sources of passive source energy to ensure energy with optimal source orientation and surface-wave characteristics were captured for each line. Surface waves were recorded with frequencies as low as 4 hertz (Hz) representing an average maximum depth of investigation between 65 meters (m) to 85 m, which represents a depth of more than 50 m below the bedrock surface in many places.

Since shear modulus is the ratio of stress over strain and shear-wave velocity is a function of shear modulus and density, it is possible to estimate relative stress of overburden rocks (shear modulus) from shear-wave velocity values. Local increases in shear-wave velocity above background and without changes in lithology can be equated to increases in stress associated with changes in distribution of the loading of overburden roof rocks above dissolution jugs. Relative shear-wave velocity lows may be associated with remnants of a partial or incremental collapse whose vertical movement has been arrested by bulking, reducing overburden stress distribution to within roof rock strength, or changes in strength with vertical migration due to an encounter with different geologic features and properties related to natural variation in deposition or erosion.

Five wells were selected for this follow up survey due to notable changes in overburden characteristics observed in the December 2019 data set. Shear-wave velocity directly over or in proximity to wells 15B and 59 in this August 2020 study represents natural geologic conditions and a normal stress regime. Overburden materials above wells 2A, 7A, and 4A still exhibit notable variability in overburden characteristics inconsistent with the native rocks.

- Wells 7A and 4A: bulk velocity of the shale bedrock is 15% higher in the current measurement compared to 2018 or 2019. A new region of lower velocity is also present on the westside of well 7A between 50-70 m depth where the signal-to-noise ratio of the fundamental mode dispersion curve was high. The overall velocity conditions in 2020 are

consistent with 2017, but 2017 was noted as possessing a zone of slightly elevated velocity. These observations may suggest a cyclic change in material strength or load distribution that has gradually changed over the last three surveys.

- Well 2A: The bulk velocity observed across lines 10 and 11 exhibits dynamic conditions with limited depth of investigation at stations in proximity to well 2A in comparison to previous surveys. In particular, shear-wave velocity was 10% lower on the eastside of well 2A and 7% lower on the northside of well 2A. These velocity variations form a dome-shaped velocity anomaly from 50-70 m depth which suggests the possibility of continued cyclic stress behavior as observed in previous years. Low velocity measurements are likely indicative of a relaxation roof failure already occurred below these low velocity areas.

Introduction

Material properties (specifically stress accumulations) measured as a function of depth above abandoned salt jugs in Hutchinson, Kansas, appear related to the mobility and upward migration of load density associated with the tensional dome of these jugs. Localized escalation in stress (as indicated by increased shear-wave velocity) above subterranean voids is one indicator of an increased potential for roof failure and void migration (Eberhart-Phillips et al., 1989; Dvorkin et al., 1996; Khaksar et al., 1999; Sayers, 2004). Previous studies, using both active and passive seismic wavefield characteristics, suggest perturbations in the shear-wave velocity field immediately above voids can be correlated to characteristics of the unsupported roof spans of salt jugs in the Hutchinson area (Sloan et al., 2010).

The strength of individual rock layers can be qualitatively described in terms of stiffness/ rigidity and empirically estimated from relative comparisons of shear-wave velocity measurements. Shear-wave velocity is directly proportional to stress and inversely related to non-elastic strain. Since the shear-wave velocity of earth materials changes when stress and any associated elastic strain on those materials becomes "large," it is reasonable to suggest load-bearing roof rock above mines or dissolution voids may experience elevated shear-wave velocities due to loading between pillars or, in the case of voids, loading between supporting side walls. This localized increase in shear velocity is not related to increased strength but to increased load as defined by Young's Modulus. High-velocity shear-wave "halos" encompassing low-velocity anomalies are suggested to be key indicators of near-term roof failure. All these phenomena have been observed within the overburden above voids in the Hutchinson Salt Member in Hutchinson at depths greater than 30 m below the bedrock surface.

Previous research projects at the Carey Boulevard Research Area (CBRA) correlated measured shear-wave velocities with the condition of dissolution voids and the physical properties of the overburden at selected locations on Vigindustries legacy solution mining property in Hutchinson. In 2008, active seismic reflection was used to evaluate the effectiveness of shear-wave velocity to estimate local stress above voids of the size and depth prevalent at the Vigindustries site. It was determined that the integrity of the overlying strata could be reasonably estimated using shear-wave seismic imaging. The lack of necessary ultra-low-frequency surface waves in the recorded wavefield have negated attempts to use active-source multi-channel analysis of surface waves (MASW) to estimate shear velocity in the lithified rocks near the top of bedrock (Miller et al., 2009).

Uncontrolled local industrial and transportation activities represent sound sources that have produced necessary low frequencies and, when recorded and processed using passive

methods, have extended the imaging depth to more than 60 m (Miller, 2011). Key to this method is the ability to estimate shear-wave velocities to depths more than double those possible using standard active sources at any particular site (Park et al., 2004). Results of passive MASW studies near this site suggest that this method is effective in identifying jugs with heightened risk for upward migration (Miller, 2011; Ivanov et al., 2013).

Following the active seismic imaging study in 2008, several two-dimensional (2-D) passive MASW surveys have been acquired at the CBRA (Table 1). Results of these early investigations largely suggested a normal stress regime with natural geologic variation. In this midyear 2020 study, passive MASW processing resulted in 5 2-D shear-wave velocity (Vs) profiles intersecting (or in proximity to) 5 wells. Individually, each profile represents a snapshot in time. When combined with previous observations at the same locations, time-lapse analysis can be used to monitor for temporal variation in shear velocity, providing insight into relative stability and void dynamics.

Table 1. Dates of and wells evaluated during 2-D passive MASW surveys at the CBRA.

Date	Wells
August 2012	2A, 1B, 2B, 3B, 5B, 6B, 7B, 12B
October 2012	2B, 4B, 6B, 17, 45, 52, 53, 59
March 2013	2A, 4B
November 2014	2A, 3B, 4B
March 2015	1B, 2B, 3B, 6B, 8A, 8B, 10B, 11B, 12B, 13B, 14B, 15B, 17, 18, 22A, 23, 23B, 29, 30, 39, 41, 42, 44, 45, 46, 86, 87, 88, 89, 90, 92
May 2015	2A, 4B
June 2015	4A, 6B, 7A, 7B, 52, 53, 59, 60
November 2017	2A, 4A, 7A, 8A, 1B, 2B, 3B, 4B, 6B, 7B, 8B, 10B, 11B, 12B, 13B, 14B, 15B, 17, 18, 22A, 23, 23B, 29, 30, 39, 41, 42, 44, 45, 46, 52, 53, 59, 60, 86, 87, 88, 89, 90, 92
October 2018	2A, 4B
December 2018	1B, 2B, 3B, 4A, 4B, 6B, 7A, 7B, 8A, 8B,10B, 11B, 12B, 13B, 14B, 15B, 17, 18, 22A, 23B, 23, 29, 30, 39, 41, 42, 44, 45, 46, 52, 53, 59, 60, 86, 87, 88, 89, 90
December 2019	1B, 2A, 2B, 3B, 4A, 4B, 5B, 6B, 7A, 7B, 8A, 8B, 10B, 11B, 12B, 13B, 14B, 15B, 17, 18, 22A, 23B, 23, 29, 30, 39, 42, 44, 45, 46, 52, 53, 59, 60, 88, 89, 90, 92
August 2020	2A, 4A, 7A, 15B, 59

Geologic and Geophysical Setting

The Permian-aged Hutchinson Salt Member occurs in central Kansas, northwestern Oklahoma, and the northeastern portion of the Texas panhandle and is prone to and has an extensive history of dissolution and formation of sinkholes (Figure 1). In Kansas, the Hutchinson Salt Member possesses an average net thickness of 75 m and reaches a maximum of more than 150 m in the southern part of the basin. Deposition occurring during fluctuating sea levels caused numerous halite beds, 0.2 to 3 m thick, to be formed interbedded with shale, minor anhydrite, and dolomite/ magnesite. Individual salt beds may be continuous for only a few miles despite the remarkable lateral continuity of the salt as a whole (Walters, 1978).

The distribution and stratigraphy of the salt is well documented (Dellwig, 1963; Holdoway, 1978; Kulstad, 1959; Merriam, 1963). The salt reaches a maximum thickness in central Oklahoma and thins to depositional edges on the north and west, erosional subcrop on the east, and facies changes on the south. The increasing thickness toward the center of the salt bed is due to a combination of increased salt and more and thicker interbedded anhydrites. The Stone Corral Formation (a well-documented seismic marker bed) overlies the salt throughout Kansas (McGuire and Miller, 1989). Directly above the salt at this site is a thick sequence of Permian shale.

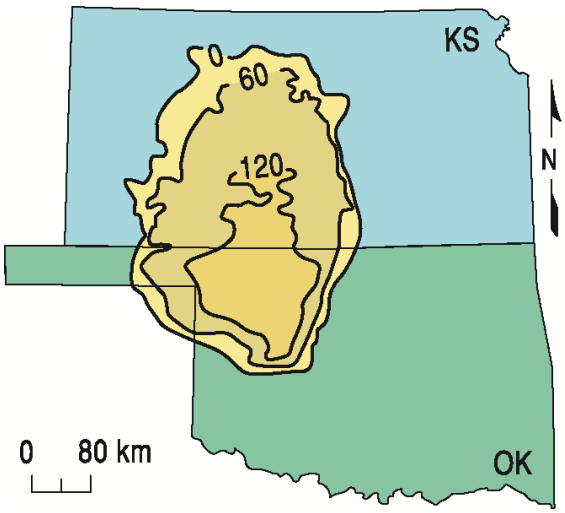

Figure 1. Approximate extent of salt formation, with contour intervals expressed in meters.

The upper 760 m of rock at this site is Permian shale (Merriam, 1963). The Chase Group (top at 300 m deep), lower Wellington Shale (top at 245 m deep), Hutchinson Salt (top at 120 m deep), upper Wellington Shale (top at 75 m deep), and Ninnescah Shale (top at 25 m deep) make up the packets of reflecting events easily identifiable and segregated within the Permian portion of the section (Figure 2). Bedrock is defined as the top of the Ninnescah Shale with the unconsolidated Pliocene-Pleistocene Equus beds making up the majority of the upper 30 m of sediment. The thickness of Quaternary alluvium that fills the stream valleys and paleosubsidence features goes from 0 to as much as 90 m, depending on the dimensions of the features.

Recent dissolution of the salt and resulting subsidence of overlying sediments forming sinkholes has generally been associated with mining or saltwater disposal (Walters, 1978). Historically, these sinkholes can manifest themselves as a risk to surface infrastructure. The rate of surface subsidence can range from gradual to very rapid. Besides risks to surface structures, subsidence features potentially jeopardize the natural segregation of groundwater aquifers, greatly increasing their potential to negatively impact the environment (Whittemore, 1989, 1990). Natural sinkholes resulting from dissolution of the salt by localized leaching within natural flow systems that have been altered by structural features (such as faults and fractures) are not uncommon west of the main dissolution edge (Merriam and Mann, 1957).

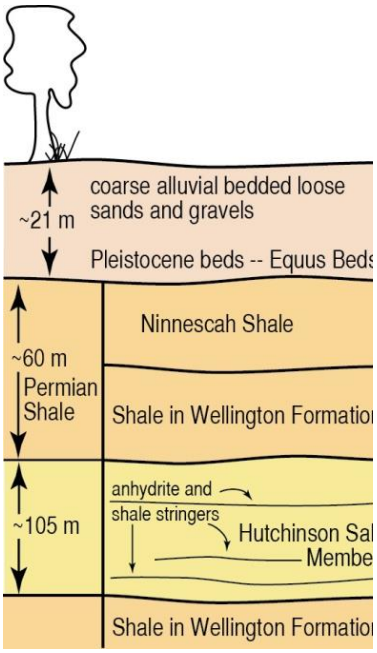

Figure 2. Generalized geology.

Caprock and its characteristics are a very important component of any discussion concerning dissolution, subsidence, and formation of sinkholes. The Permian shales (Wellington and Ninnescah) that overlay the Hutchinson Salt Member are about 60 m thick in this area and are characterized as generally unstable when exposed to freshwater, being susceptible to sloughing and collapse (Swineford, 1955). These Permian shales tend to be red or reddish-brown and are

commonly referred to as "red beds." Permian red beds are extremely impermeable to water and have provided an excellent seal between the freshwaters of the Equus beds and the extremely water-soluble Hutchinson Salt Member. The modern-day expanse and mere presence of the Hutchinson Salt is due to the protection from freshwater provided by these red beds.

Isolating the basal contact of the Wellington Formation provides key insights into the general strength of roof rock expected, if dissolution-mined salt jugs (salt jugs are the jug-shaped cavities or voids in the salt that form after salt has been dissolution mined in proximity to the wells) reach the top of the salt zone. Directly above the salt/shale contact is approximately 6 m thick dark-colored shale with joint and bedding cracks filled with red halite (Walters, 1978). Once unsaturated brine comes in contact with this shale layer, these red halite-filled joints and bedding planes are rapidly leached, leaving an extremely structurally weak layer.

Field Layout and Data Acquisition

To ensure the highest quality data, receivers were deployed during daylight hours and train data were recorded at night when cultural and industrial noise was minimal to provide optimum signal-to-noise ratio. Analysis of previous seismic energy sources captured during passive recording at this site clearly indicated trains at distances of 2 kilometers (km) or more provided the best broad spectrum, low-frequency seismic energy (Miller, 2011). Since seismic energy with characteristics best suited for this study may arrive when trains are at distances greater than can be detected by spotters, seismic energy was recorded continuously throughout the night to ensure the capture of all times possessing optimum data.

Data were acquired over one night, August 20, 2020. A total of five seismic lines (Figure 3**)** were deployed collectively during the day. Line layout was designed to cross directly over all wells of interest. A 2-D grid of receivers designed to monitor and allow determination of the incident orientation of passive seismic energy was active throughout the night as well. Seismic receivers were single ION 4.5 Hz geophones spaced at 3 m intervals. The seismic lines collectively totaled approximately 1540 m in length. The 2-D monitoring/ alignment grid consisted of 131 receivers spaced at 5 m intervals and was configured to form four concentric expanding squares with 10, 30, 50, and 70 m sides. Data were recorded with a 400+ channel 24-bit Geometrics Geode distributed seismic system. Seismic records were 30 seconds (s) long with a 2 millisecond (ms) sampling interval. In total, 971 seismic records were recorded, which resulted in 26.3 gigabytes (Gb) of data.

Processing and Analysis

Data were processed using algorithms developed at the Kansas Geological Survey (KGS). The passive method used for this study is well published and has consistently proven effective producing good-quality results (Park et al., 2004; Ivanov et al., 2013). The continuous-data-acquisition method records energy from nearby sources at various orientations with respect to the seismic line. Data from the 2-D grid are evaluated for optimized source alignment with respect to each 1-D seismic line allowing data rotation or analysis of only data from near in-line sources.

For each line, the surface-wave amplitudes recorded by the 2-D grid were plotted as phase velocity versus frequency across a range of azimuths, from 0 to 360 degrees relative to the seismic line, to identify which record had the best broad-band, low-frequency source energy with

an azimuth as near zero as possible (Figure 4). Seismograms for each line with optimum source characteristics were selected and segmented into the shortest groups of receivers ("spread length") that provided dispersion patterns on phase velocity versus frequency plots with the greatest percentage of high amplitude fundamental mode Rayleigh-wave energy and minimal higher-order surface-wave interference (Figure 5).

Figure 3. Aerial photo with GPS locations 2-D grid of receivers (yellow squares) with respect to orientation of five seismic lines and wells in the August 2020 study.

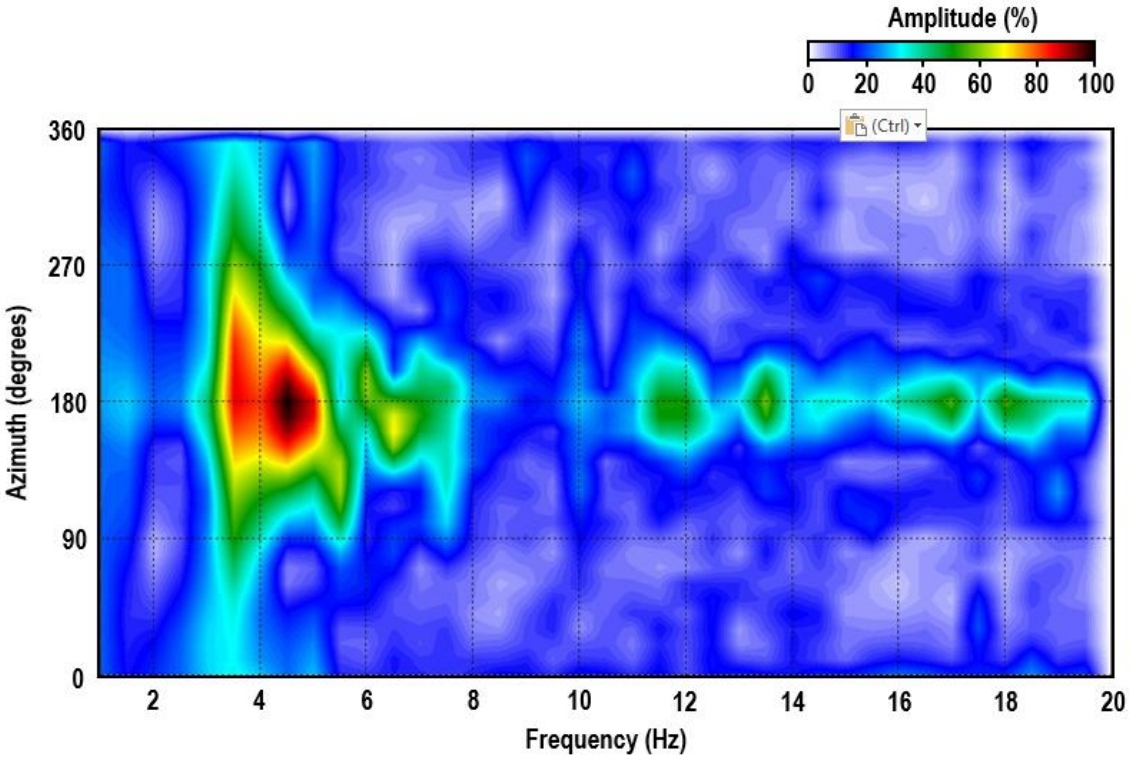

Figure 4. Azimuth plot indicating the direction of the dominant passive source energy (in degrees counter-clockwise from east). Here, the dominant passive source energy is centered on approximately 180°.

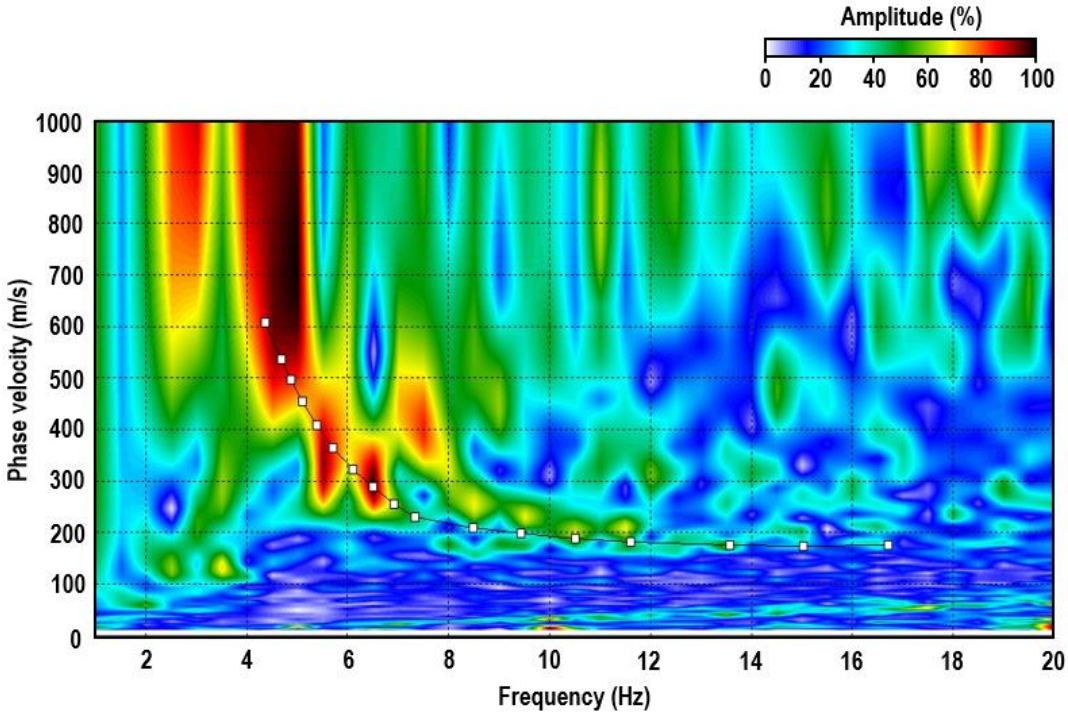

Figure 5. Dispersion pattern with high signal-to-noise ratio of the fundamental mode Rayleigh wave.

Fundamental mode dispersion curves were picked and inverted to obtain a 2-D section of shear-wave velocity as a function of depth. The apparent velocity (v_{app}) is:

$$v_{app} = \frac{v_{act}}{(\cos\theta)} \tag{1}$$

where v_{act} is the actual seismic velocity and θ is the azimuth of the source with respect to the seismic line determined from the azimuth versus frequency plot. Thus, the percent increase in velocity (Δv) is:

$$\Delta v = \frac{1}{\cos\theta} - 1 \tag{2}$$

Equation 2 was used to calculate the increase in velocity due to the source azimuth for each line (Table 2).

Table 2. Directions of the passive seismic sources and the seismic lines; spread length used for processing, the angle of the source with respect to the line (θ, in degrees counterclockwise from east), and the percent increase in apparent velocity (Δv) attributable to oblique source orientations.

	processing spread length(s)	source orientation	line orientation	θ	Δv
line 7	84 m	160°	165°	5°	< 0.38%
line 9	93 m	100°	86°	14°	< 3.06%
Line 10	84 m	180°	180°	0°	0%
Line 11	78 m	95°	74°	21°	7.11%
line 13	84 m	163°	172°	9°	< 1.25%

Results and Observations

Line 7

The central section of Line 7, oriented NW-SE, extends across well 15B located approximately at station 7024 (Figure 6); well 15B was located below station 7071 in 2018 (Figure 6a) and 2019 (Figure 6b). The upper 15 m of the ground surface has an average shear-wave velocity of 175 m/s, which is consistent with unconsolidated/alluvial materials in this area. The top of bedrock is indicated by the large velocity gradient at approximately 15 m depth. An 84 m spread was selected for processing in August 2020, consistent with the previous acquisition in 2019. The bulk-velocity trend in 2020 remained relatively consistent from NW to SE across the surveyed area with an average depth of investigation of 55 m; the top of the Wellington Shale Formation is at 55-60 m depth. Fundamental-mode phase-velocities were slightly higher on the westside of well 15B compared to the eastside due to a change in frequency content. Overall, the bulk-velocity trend observed in 2020 (Figure 6c) is generally consistent with previous years (Appendix A1), although greater inverted depth was achieved in 2018 (Figure 6a) and 2019 (Figure 6b), which is a function of source energy.

Dispersion curves plotted in Figure 7 demonstrate the varied fundamental-mode trends from 2018 to 2020 near well 15B. The fundamental mode in 2020 remained relatively unchanged since 2019 with similar frequency content from 4-18.5 Hz. Phase velocities corresponding to the fundamental mode were slightly higher in 2020 compared to 2019. Nonetheless, the average velocity in 2020 remained within 5% of the average velocity calculated in 2019 for 15-60 m depth. Velocity information for depths greater than 60 m were not inverted due to limited signal below 4 Hz, including the eastside of well 15B where velocity was 10% lower in 2019 than in 2018.

Line 9

N-S oriented Line 9 runs parallel to Williams Street and intersects wells 52, 53, 59, and 60. In this follow up survey, a portion of Line 9 was deployed to focus the investigation on well 59, which the line crosses at station 9030 (Figure 8c); Line 9 crossed well 59 at approximately station 9098 in 2018 and 2019. The upper 15 m has an average shear-wave velocity of 175 m/s, which is consistent with the expected conditions at this site and previous survey estimations (Appendix A2). Bulk velocity of the upper 60 m was 10% lower in midyear 2020 (Figure 8c) compared to the 2019 survey (Figure 8b); average depth of investigation was also 20 m shallower in midyear 2020 compared to 2019. Despite this lower velocity trend, the 2020 result is generally consistent with the 2018 (Figure 8a) and all previous years at depths below 50 m; therefore, elevated velocity was only been observed in 2019 around well 59 and currently the stress seems to have returned to native for the overburden at this well. It is likely that the stress build up during 2019 was relieved over the 9 months between the two surveys.

Fundamental modes from 2018, 2019, and midyear 2020 (Figure 9) exhibited similar phase velocities trends above 6 Hz with greater variability between 4-6 Hz. Phase velocities below 6 Hz varied by 10-15% with the midyear 2020 fundamental-mode having the lowest phase velocities. The change in maximum depth of investigation is the result of these varying fundamental-mode trends from year to year. In 2019, the fundamental-mode trend was noted as possessing decreased energy amplitudes throughout line 9 with low coherency observed at stations surrounding well 59 (Figure 10a). Signal quality is higher in the midyear 2020 data set (Figure 10b), but it is important to also note the higher modes exhibit the same phase velocity

and frequency characteristics as the fundamental mode observed in 2019. The presence of higher modes, much like the 2019 elevated velocity, may be an indication of heterogeneity in the shallow subsurface. Therefore, continued monitoring is recommended. Although the 2020 bulk-velocity trend is within range of native geologic materials, additional surveying is suggested to monitor for more intermittent temporal changes.

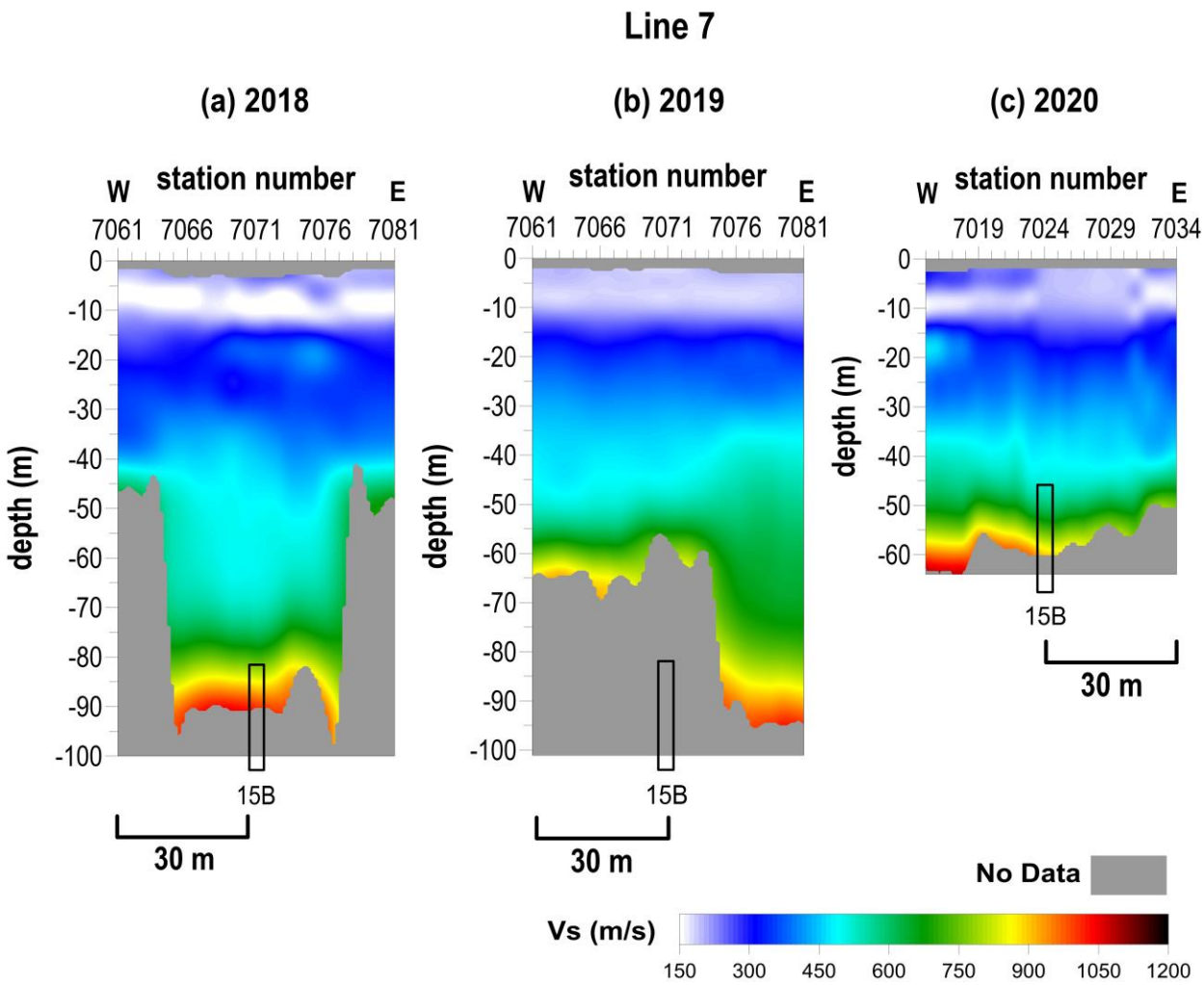

Figure 6. Shear-wave velocity profiles from line 7 from (a) December 2018, (b) the December 2019, and (c) the current August 2020 investigation with approximate well locations.

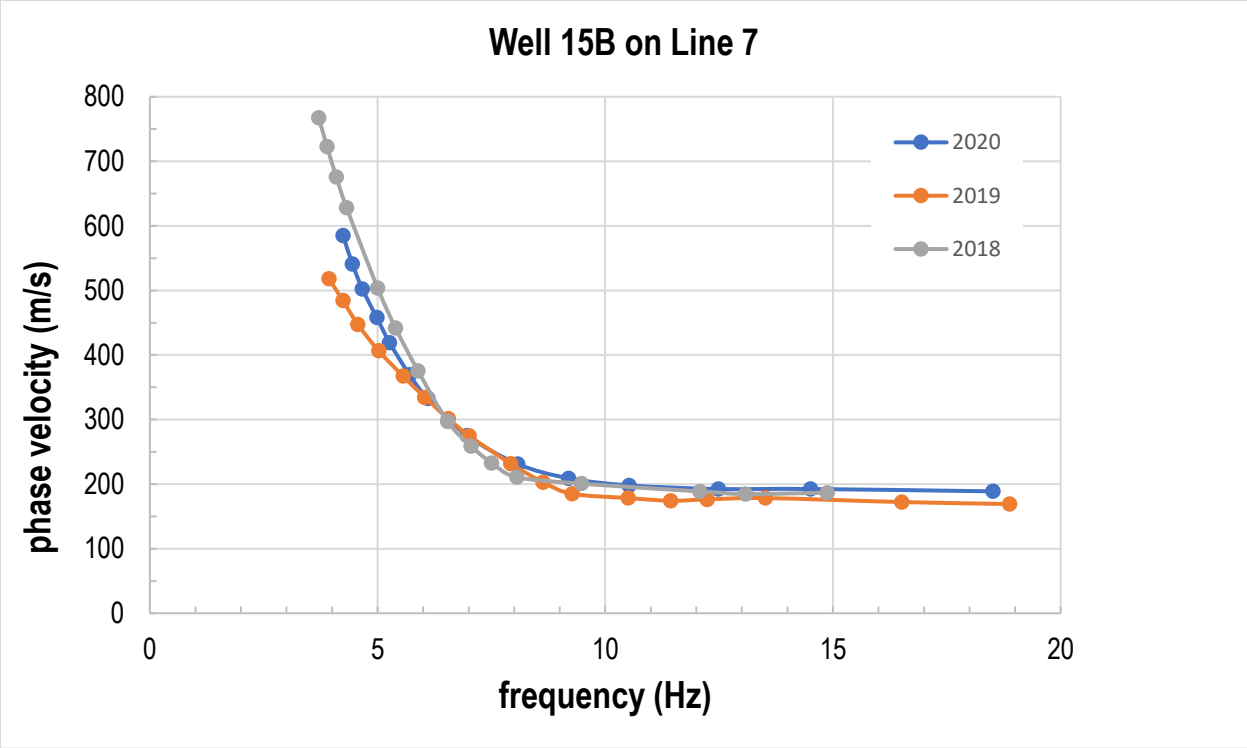

Figure 7. Dispersion curves from line 7 from (a) December 2018, (b) the December 2019, and (c) the current August 2020 investigation with approximate well locations.

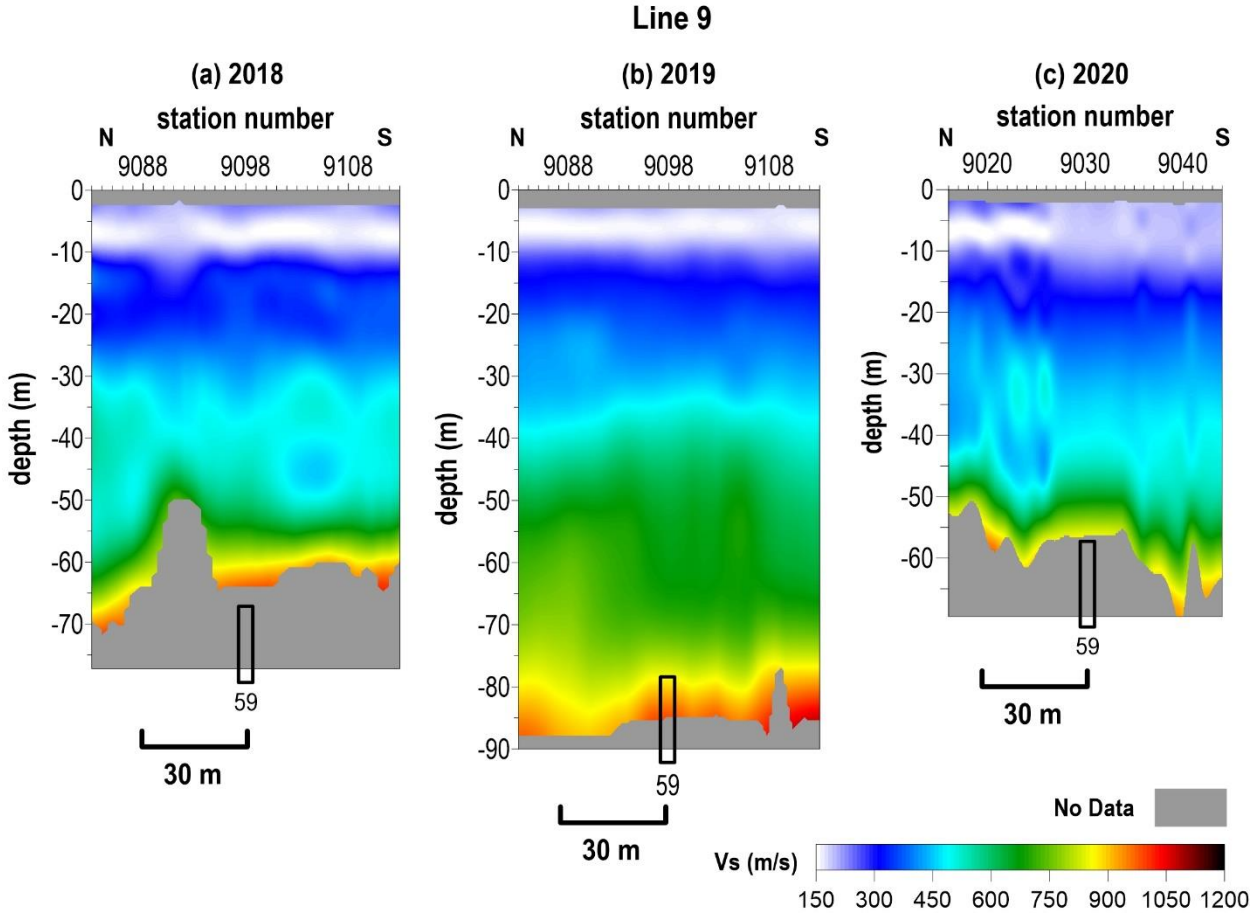

Figure 8. Shear-wave velocity profiles from line 9 from (a) December 2018, (b) December 2019, and (c) the current August 2020 investigation with approximate well locations.

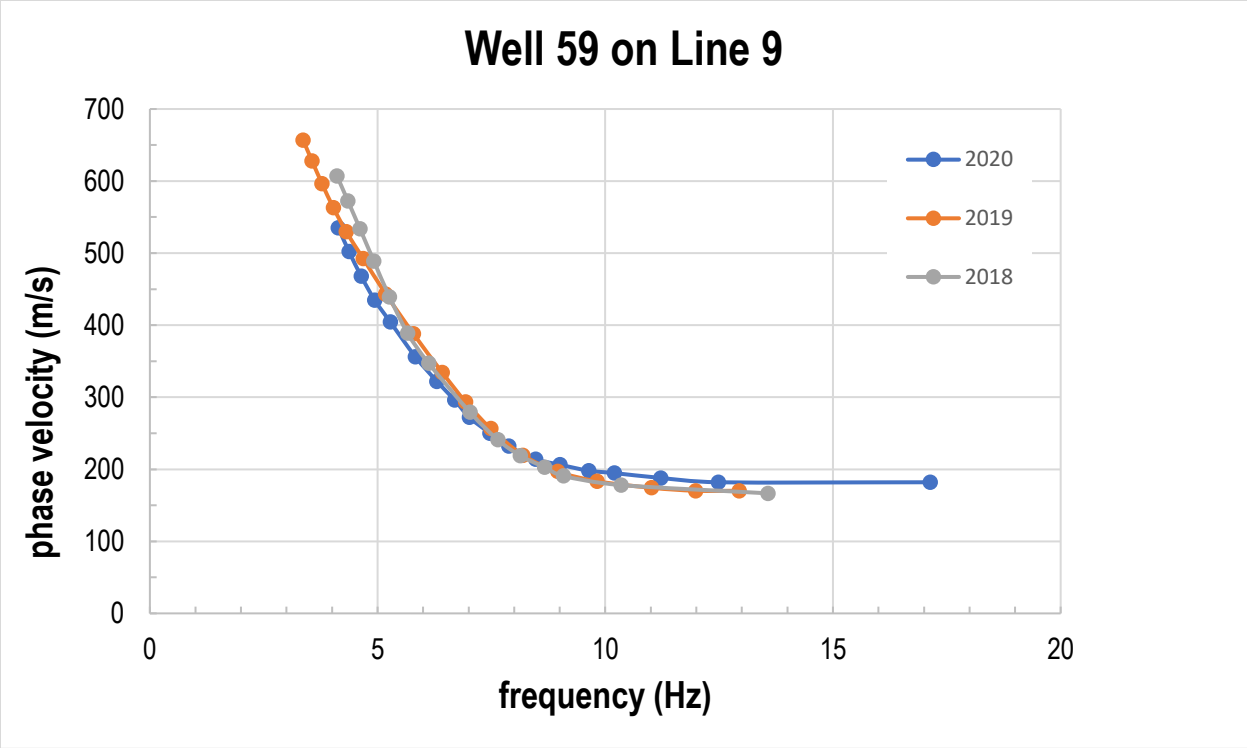

Figure 9. Dispersion curves from line 9 from (a) December 2018, (b) December 2019, and (c) the current August 2020 investigation with approximate well locations.

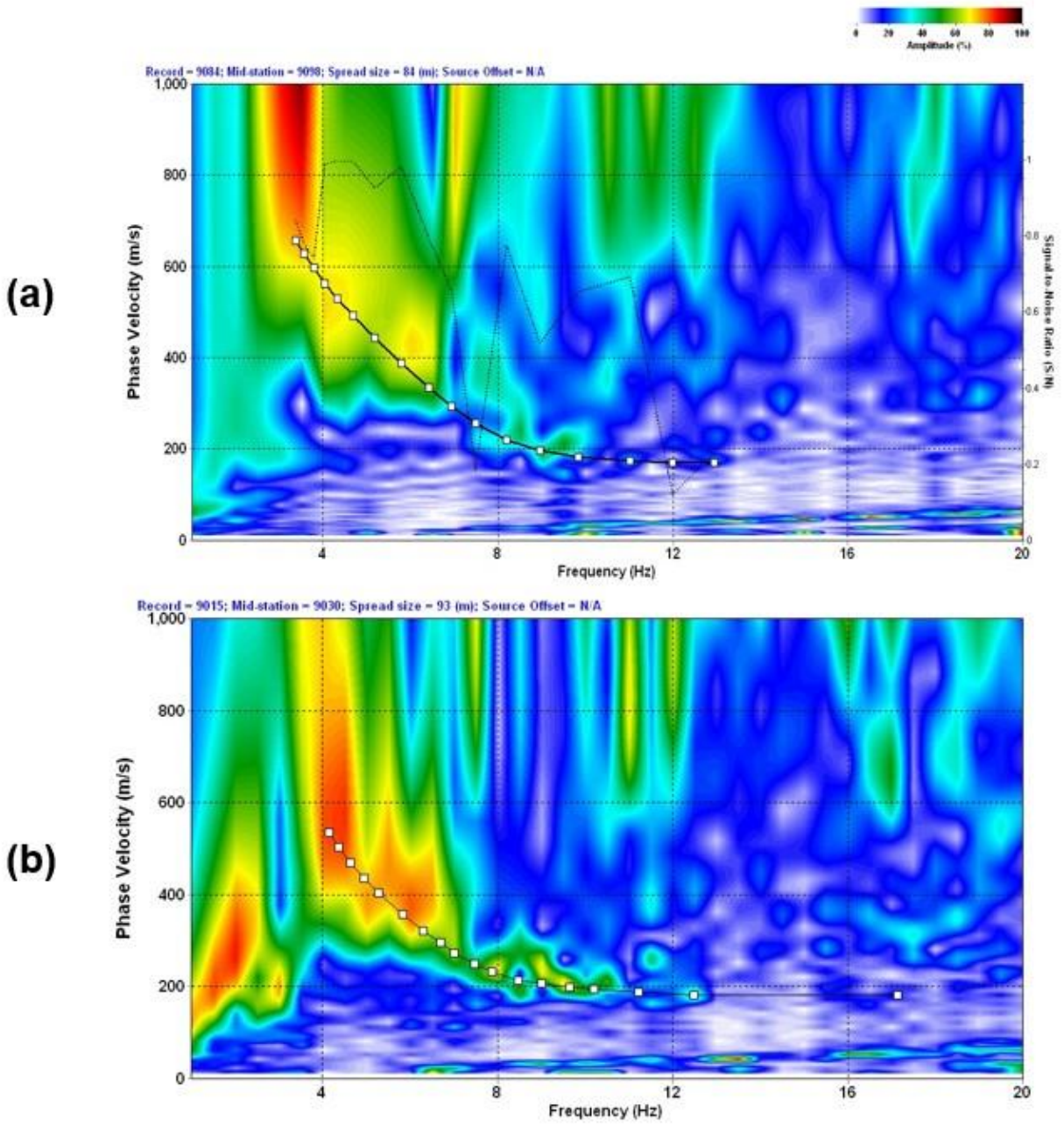

Figure 10. Dispersion curves images for well 59 on line 9 from (a) December 2019 and (b) the current August 2020 investigation. Signal quality was lower in 2019 compared to 2020.

Line 10 and Line 11

Line 10 is a W-E oriented line that crosses well 2A at station 1024.5 (Figure 11); in 2018 and 2019, line 10 crossed well 2A at station 1022.5. The average velocity of the upper 15 m is approximately 175 m/s, consistent with the unconsolidated/alluvial sediment expected in this area. The velocity gradient at 15 m indicates the interface between the unconsolidated sediment and shale bedrock. Depth of investigation was limited between stations 1029-1022 forming a dome-shaped anomaly with elevated velocity centered on well 2A. Furthermore, a region of anomalously low velocity is observed east of well 2A from 55-80 m depth. Stations west of station 1029 exhibit velocities consistent with previous years and the expected geologic conditions, whereas stations east of station 1029 at equivalent depths are approximately 25% lower than normal.

Multiple, overlapping and competing fundamental modes were observed at frequencies below 7 Hz at western stations. These two unique fundamental mode curves merge together into a single mode towards eastern stations. These multiple modes could not be reduced using advanced filtering techniques because both modes were high-amplitude and exhibited similar phase velocities. This multi-mode behavior suggests heterogeneity at deeper depths where multiple stress states may exist within the shale bedrock. These asymmetric conditions are similar to the 2015 survey (Appendix A3) where greater depth of investigation and a region of lower velocity were also observed on the east side of well 2A. This suggests the continuation or repeat of stress field behavior likely associated with load redistribution in the shale caprock following a localized failure event.

Line 11 (Figure 12c), oriented N-S over well 2A exhibits velocity conditions similar to Line 10 including varied depth of investigation on one side of the well and elevated velocity at stations surrounding the well; Line 11 crosses well 2A at station 1024. These asymmetric velocity conditions are consistent with previous observations (Appendix A4) where the northern side of well 2A exhibited greater depth of investigation and slightly reduced velocity compared to the southern side of well 2A. Overall, the velocity conditions observed on Lines 10 and 11 (Appendices A3, A4) suggest another failure event (stress release) may have occurred following the same asymmetric mechanical behavior at well 2A as observed previously.

Line 13

Line 13 is oriented W-E and intersects wells 7A and 4A located approximately at stations 1328 and 1376.5 respectively (Figure 13). The upper 15 m has an average shear-wave velocity of 175 m/s, which is consistent with unconsolidated materials across this area. The bedrock surface is observed at approximately 15 m depth as indicated by the large velocity gradient. Bulk velocity across Line 13 in 2020 (Figure 13d) is nearly 15% higher than either the 2018 (Figure 13b) or 2019 (Figure 13c) surveys; however, the 2020 midyear survey result is generally consistent with the 2017 findings. It is interesting to note in general, surveys with depth of investigation greater than 60 m (i.e., 2017, 2020) yielded elevated bulk velocity compared to surveys where depth of investigation was limited to 50-60 m depth (i.e., 2018, 2019). Although velocities are considered elevated in the midyear 2020 and 2017 results, bulk velocities are comparable to estimates from other survey lines at this site that report velocities considered within the normal range for the local geologic materials.

Interestingly, dispersion curves with the highest coherency were observed east of well 4A and west of well 7A. For stations at and between these wells, the fundamental mode was less continuous and exhibited lower energy amplitudes; the fundamental mode was still interpreted

with high confidence despite these factors. An interfering higher mode was observed at westernmost stations where the average velocity between 50-80 m was also slightly lower than surrounding measurements. This yielded greater depth of investigation for stations west of well 7A; a similar observation was made in 2017, in contrast to stations at and east of well 7A. This higher mode arrival in the midyear 2020 survey became the dominant trend across stations between the two wells after the fundamental and higher mode merged together. Such behavior (e.g. merging modes) has been associated with heterogeneity in the subsurface; heterogeneity in this case may be indicative of changes in the shale bedrock competency. Based on studies over the last five years, the 2017 and midyear 2020 studies exhibit an elevated bulk-velocity structure compared to 2015, 2018, and 2019 (Appendix A5). Overall, it is recommended that monitoring continue over these wells to further evaluate whether velocity variations are indicative of changes/cycles in situ conditions or varying signal quality.

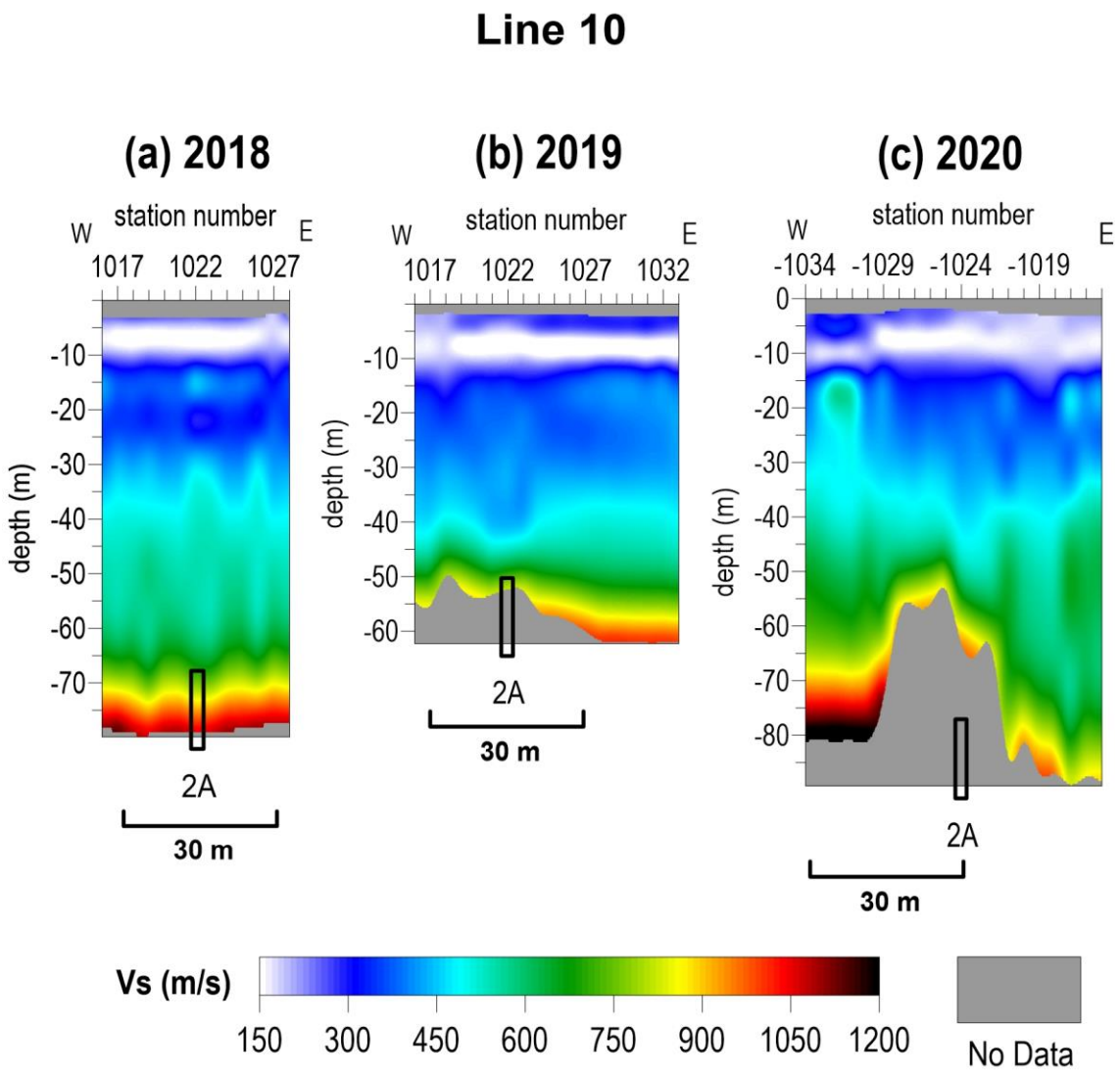

Figure 11. Shear-wave velocity profiles from line 10 from (a) October 2018, (b) the December 2019, and (c) the current August 2020 investigation with approximate well locations.

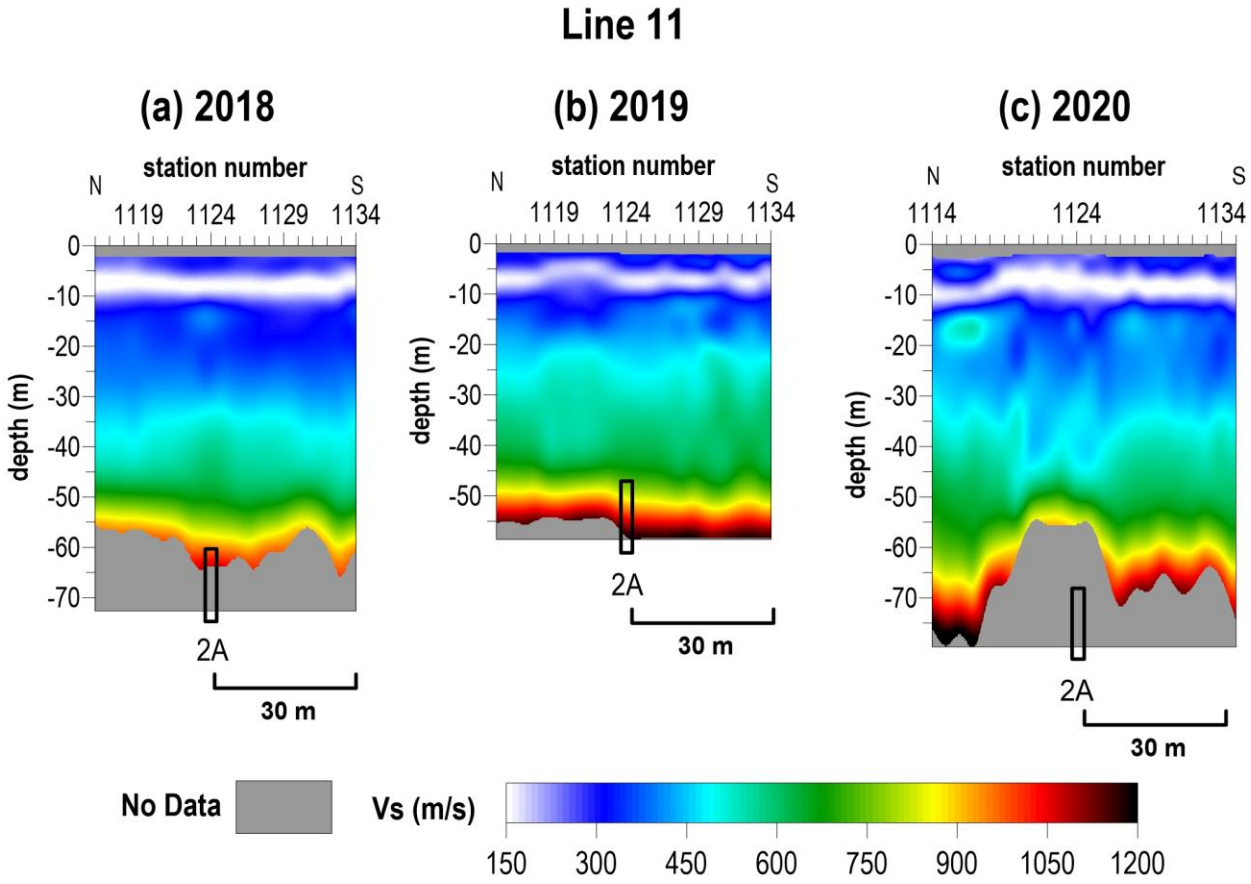

Figure 12. Shear-wave velocity profiles from line 11 from (a) October 2018, (b) December 2019, and (c) the current August 2020 current investigation with approximate well locations.

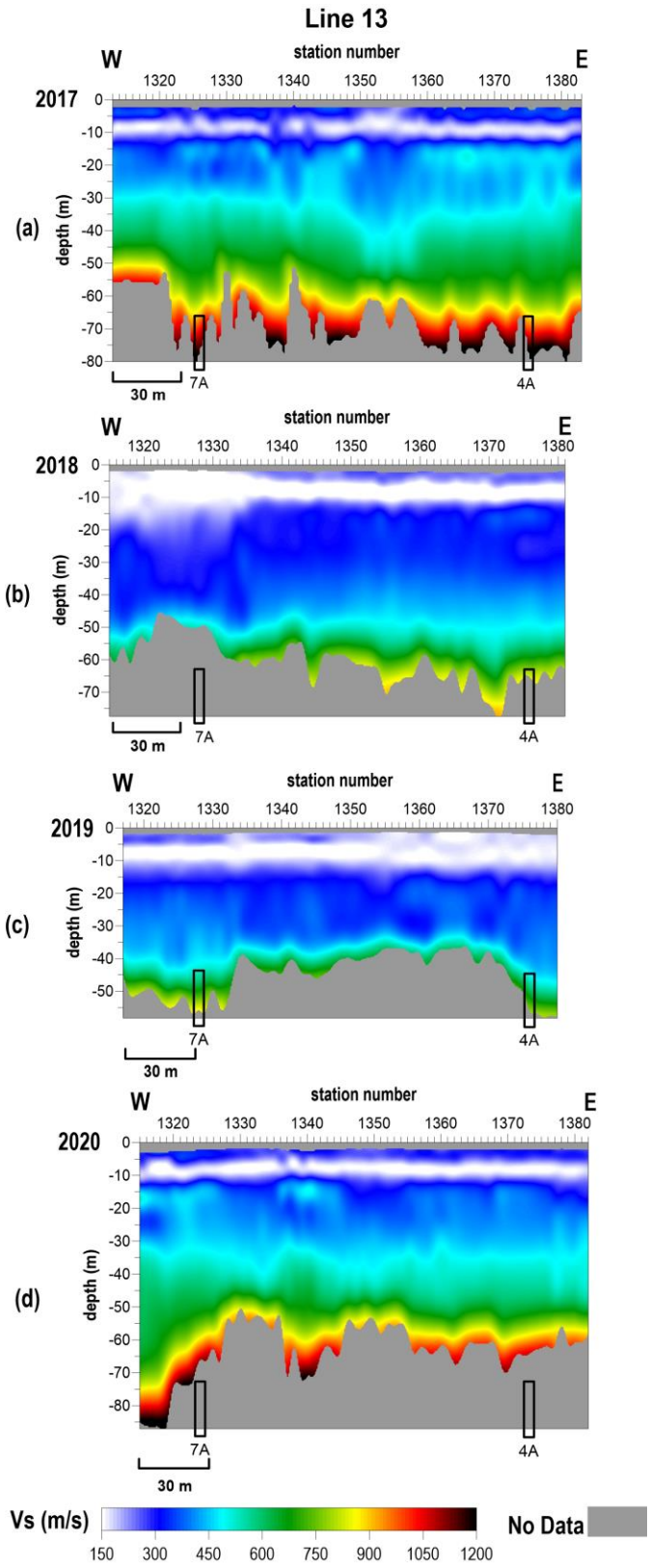

Figure 13. Shear-wave velocity profiles from line 13 from (a) November 2017, (b) December 2018, (c) December 2019, and (d) the current August 2020 investigation with approximate well locations.

Interpretation and Discussion

Wells with conditions of normal stress regime, and consistent surface-wave behavior

Well 15B:

Bulk-velocity conditions remain consistent with the 2019 survey. In midyear 2020, low-frequency signal was limited again at stations in the location of well 15B, with an abrupt increase in inverted depth east of the well; this is consistent with 2019 observations. It is not clear if this observation is a direct indication of varied shale competency, but this region should remain under observation since shear-wave velocity was 5% lower in midyear 2020, compared to 2019 east of the well.

Well 59:

The midyear 2020 result is generally consistent with 2018 calculated values and all previous years; bulk velocity was only reported as elevated in 2019. Fundamental modes from 2018, 2019, and midyear 2020 exhibited similar phase velocities between 4-14 Hz. In 2019, frequencies as low as 3 Hz were available resulting in greater depth of investigation (80 m) compared to 2018 and midyear 2020 (~65 m); depth of investigation increases when lower frequency signal is available. The presence of higher modes in 2020, much like the 2019 elevated velocity, may be an indication of heterogeneity in the shallow subsurface. Lower frequency content in the midyear 2020 data set would have been favorable for a more enhanced interpretation of the anomalous velocity region observed in 2019 near well 59. Nonetheless, bulk-velocity conditions measured in August 2020 represent the natural geologic conditions and suggest a normal stress regime.

Wells with conditions of normal stress regime, but varying surface-wave behavior

Wells 7A and 4A:

At depths greater than 30 m, bulk velocity is 15% higher in the midyear 2020 calculations compared to 2018 and 2019. A new region of lower velocity is also present on the westside of well 7A between 50-70 m depth where the signal-to-noise ratio of the fundamental mode was high in the midyear 2020 data set. The overall velocity estimates in midyear 2020 are consistent with those observed in 2017. Since 2017 was noted for slightly elevated velocity, these observations may suggest a change in stress conditions (e.g., loading changes) that has gradually increased over the last three surveys.

Wells with possibly varying stress regime

Well 2A:

The bulk velocity observed across Lines 10 and 11 are suggestive of dynamic conditions with limited depth of investigation near well 2A when compared to previous survey data. In particular, shear-wave velocity was 10% lower on the eastside of well 2A and 7% lower on the northside of well 2A in comparison to the 2019 survey. Mapping these velocity variations produced a dome-shaped velocity anomaly from 50-70 m depth unique to velocity conditions surrounding the well. Away from the well, velocity values lack symmetry relative to the well location. This suggests the overburden at the well site could be experiencing a cyclic stress behavior consistent with what has been observed when comparing velocity images from previous years.

Conclusions

This midyear 2020 survey was undertaken as a result of observations and associated recommendations made following acquisition, processing, and interpretation of the routine annual survey completed in December of 2019 at the Hutchinson CBRA site (Morton et al., 2020). Shear-wave velocity images from four different well groupings on December 2019 data have anomalies sufficiently outside the normal range with associated error bars to justify an increased awareness and monitoring. Strength characteristics deduced from shear-wave velocities derived from the passive MASW surveys around wells 2A (Lines 10 and 11), 4A and 7A (Line 13), 15B (Line 7), and 59 (Line 9) indicated change consistent with either increasing stress or recent stress release suggestive of a relaxed or degraded state. These five wells represent the most likely threat to ground stability from the December 2019 survey.

The overburden measurements of shear velocity made during the 2019 survey across these four lines suggested stress conditions above the five wells were sufficiently outside the range of 'expected' since the 2018 survey to justify intermediate measurements in advance of the normal annual measurement program. The type of change observed over these five wells dictated the need for a midyear survey prior to the November/December 2020 annual survey to better understand and estimate rate, consistency, and extent of this observed change. Shear velocities above and in close proximity to wells 15B, 59, 7A, 4A, 2A were inconsistent with previous years or deviated from expected trends established from multiple years of measurements. These interpretations and observations on 2019 survey data prompted a midyear survey in 2020 to provide confidence in velocity trend progression and identify any changes in the established subsidence threats.

Shear-wave velocity profiles calculated from the four lines traversing the five wells during the August 2020 survey were interpreted and classified into three different categories. These categories were based on measurements and wave observations in overburden above and in proximity to the well. They are normal stress regime and well-behaved surface wave propagation, normal stress regime and inconsistent surface wave behavior, and changes in stress regime.

Based on comparison of August 2020 and December 2019 data, the shear velocity structures and properties in overburden at wells 15B and 59 appear to be consistent with what is considered native for undisturbed rock and soil in the upper 80 m at this site. Irregularities observed on data from the December survey were isolated and resolved with the data acquired during August. A similar increase in shear velocity above well 59 was observed in the 2015 data but was not present on the 2016 annual survey. This would lead us to believe that the void roof in well 59 is slowly migrating toward the surface with failure occurring on about a 4- or 5-year cycle, but to date has not reached the dolomite. The August follow up survey was an outstanding tool for confirmation of consistent development and identifying any potentially threatening subsurface conditions. These wells are categorized as within a normal stress regime and well-behaved surface wave propagation patterns.

Results of the August 2020 acquisition and processing of data traversing wells 4A and 7A are consistent with a cyclic stress environment and an irregular surface wave propagation pattern. Elevated shear velocity below the bedrock surface is consistent with the 2017 survey over these wells. The 2017 survey was considered natural for this area with the 2018 and 2019 velocity measurements being abnormally low. It is reasonable to suggest that as of August of 2020 the

velocity regime above these two wells has rebounded and returned to more of a native state after rebounding from 15% below normal velocities during 2018 and 2019.

Consistent with most of the previous surveys the shear-wave velocity structure above and around well 2A is irregular and variable between surveys. After more than a half dozen surveys acquired over well 2A the stress/shear velocity distribution is becoming more familiar. The shape of the tensional dome is consistent with physical models with the asymmetric distribution of low and high shear velocities relative to native in these sediments. Changes in shear velocity should be expected around well 2A and is likely related to changes in the roof of the salt jug or a possibility that we are investigation is surface loading. With the proximity of the grain elevators and normal operating procedures that would include the filling and emptying of those tanks, surface loading could be stressing the ground surface sufficiently to change the sub-bedrock surface stress regime. Modeling will be undertaken to establish if differential loading of the ground surface could affect the kind of changes we are measuring around 2A.

Recommendations

Seismic surveys at the CBRA over the last 15 plus years have provided insights and resolved some critical questions related to ground stability and the vertical migration of voids remaining from legacy salt solution mining that began almost a century ago. Clearly, passive surveying in this area is the most cost-effective way to confidently monitor change in the upper 70–80 m potentially related to vertical migration of voids toward the ground surface. Five areas associated with locations of legacy solution wells were identified by the 2019 survey with characteristics that justify an intermediate (6 month) monitoring survey. Wells 2A, 4A, 7A, 15B, and 59 have been identified on 2019 data as possessing characteristics inconsistent with "native" shear-wave velocity measurements or with calculated shear velocities different from years past. This intermediate survey confirmed the historical pattern and supports continued monitoring at the current levels.

To that end, sediments around well 2A appear to possess the most dynamic shear velocity distributions on surveys over the last several years. Consistent changes have been observed in each of the last three years (2017, 2018, and 2019). Considering the most significant changes are occurring at depths greater than 50 m, this location does not represent an imminent threat for surface subsidence. However, this much change in shear velocity year to year does indicate either a void roof that is actively failing or irregular surficial loading is stressing the overburden. Key with well 2A is detecting any increase in shear velocity at or near the bedrock surface. Regardless of the source, that would signal the point where more invasive measures might be necessary to arrest any changes in material properties migrating to the surface. Continued monitoring on annual or shorter intervals will provide the necessary confidence in annual recommendations.

August 2020 data acquired over well 4A and 7A supports the suggestion that the velocities measured during the 2019 survey are consistent with those recorded in 2015 and the overburden has returned to 2016-2018 stress levels. The 2019 reduction in shear velocity is strong evidence supporting a cyclic pattern that had been suggested as indicative of the presence of a void that has migrated into the shale but still well below the dolomite. These data from midyear 2020 support the need to continue monitoring annually with the expectation of these cycles in shear velocity to continue as long as the void has not filled with collapse breccia and

continues moving toward the ground surface. The proximity of well 7A to the north boundary also supports continuing to monitor this area.

Data acquired over well 15B from the August 2020 survey is interpreted to be consistent with a roof fall periodicity and provides a reasonable measure of the rate of void migration. Considering the angle of draw and proximity of the west property line, annual monitoring is still a good way to keep track of void migration at this well. This midyear data set has addressed the question raised as a result of the annual 2019 survey and instills confidence that the current program is prudent and effective in managing the response to any void dynamics at this site.

References

Davies, W. E., 1951, Mechanics of Cavern Breakdown. Bulletin of the National Speleological Society, no. 13, 36-43.

Dellwig, L.F., 1963, Environment and mechanics of deposition of the Permian Hutchinson Salt Member of the Wellington shale: Symposium on Salt, Northern Ohio Geological Society, p. 74-85.

Dvorkin, J., A. Nur, and C. Chaika, 1996, Stress sensitivity of sandstones: *Geophysics*, v. 61, p. 444-455.

Eberhart-Phillips, D., D.-H. Han, and M.D. Zoback, 1989, Empirical relationships among seismic velocity, effective pressure, porosity, and clay content in sandstone: *Geophysics*, v. 54, p. 82-89.

Holdoway, K.A., 1978, Deposition of evaporites and red beds of the Nippewalla Group, Permian, western Kansas: Kansas Geological Survey Bulletin 215.

Ivanov, J., R.D. Miller, S.L. Peterie, J.T. Schwenk, J.J. Nolan, B. Bennett, B. Wedel, J. Anderson, J. Chandler, and S. Green, 2013, Enhanced passive seismic characterization of high priority salt jugs in Hutchinson, Kansas: Preliminary report to Burns & McDonnell Engineering Company.

Khaksar, A., C.M. Griffiths, and C. McCann, 1999, Compressional- and shear-wave velocities as a function of confining stress in dry sandstones: *Geophysical Prospecting*, v. 47, p. 487-508.

Kulstad, R.O., 1959, Thickness and salt percentage of the Hutchinson salt; *in* Symposium on Geophysics in Kansas: Kansas Geological Survey Bulletin 137, p. 241-247.

McGuire, D., and B. Miller, 1989, The utility of single-point seismic data; *in* Geophysics in Kansas, D.W. Steeples, ed.: Kansas Geological Survey Bulletin 226, p. 1-8.

Merriam, D.F., 1963, The Geologic History of Kansas: Kansas Geological Survey Bulletin 162, 317 p.

Merriam, D.F., and C.J. Mann, 1957, Sinkholes and related geologic features in Kansas: *Transactions of the Kansas Academy of Science*, v. 60, p. 207-243.

Miller, R.D., 2011, Progress report: 3-D passive surface-wave investigation of solution mining voids in Hutchinson, Kansas: Interim report to Burns & McDonnell Engineering Company, January, 9 p.

Miller, R.D., J. Ivanov, S.D. Sloan, S.L. Walters, B. Leitner, A. Rech, B.A. Wedel, A.R. Wedel, J.M. Anderson, O.M. Metheny, and J.C. Schwarzer, 2009, Shear-wave study above Vigindustries, Inc. legacy salt jugs in Hutchinson, Kansas: Kansas Geological Survey Open-file Report 2009-3.

Morton, S., L., S. Peterie, J. Ivanov, R. Miller, B. Bennett, C. Bunker, K. Burke, E. Knippel, J. Lawler, C. Umbrell, and B. Wedel, 2020, Passive Seismic Characterization of High Priority Salt Jugs Near Hutchinson, Kansas: December 2019, Kansas Geological Survey Open-file Report 2020-15, 39 p.

Park, C., R. Miller, D. Laflen, N. Cabrillo, J. Ivanov, B. Bennett, and R. Huggins, 2004, Imaging dispersion curves of passive surface waves [Exp. Abs.]: Annual Meeting of the Soc. of Expl. Geophys., Denver, Colorado, October 10-15, p. 1357-1360.

Sayers, C.M., 2004, Monitoring production-induced stress changes using seismic waves [Exp. Abs.]: Annual Meeting of the Soc. of Expl. Geophys., Denver, Colorado, October 10-15, p. 2287-2290.

Sloan, S.D., S.L. Peterie, J. Ivanov, R.D. Miller, and J.R. McKenna, 2010, Void detection using near-surface seismic methods; *in* Advances in Near-Surface Seismology and Ground-Penetrating Radar, SEG Geophysical Developments Series No. 15, R.D. Miller, J.D. Bradford, and K. Holliger, eds.: Tulsa, Society of Exploration Geophysicists, p. 201-218.

Swineford, A., 1955, Petrography of upper Permian rocks in south-central Kansas: State Geological Survey of Kansas Bulletin 111, 179 p.

Walters, R.F., 1978, Land subsidence in central Kansas related to salt dissolution: Kansas Geological Survey Bulletin 214, 82 p.

Whittemore, D.O., 1990, Geochemical identification of saltwater contamination at the Siefkes subsidence site: Report for the Kansas Corporation Commission.

Whittemore, D.O., 1989, Geochemical characterization of saltwater contamination in the Macksville sink and adjacent aquifer: Kansas Geological Survey Open-file Report 89-35.

Appendix

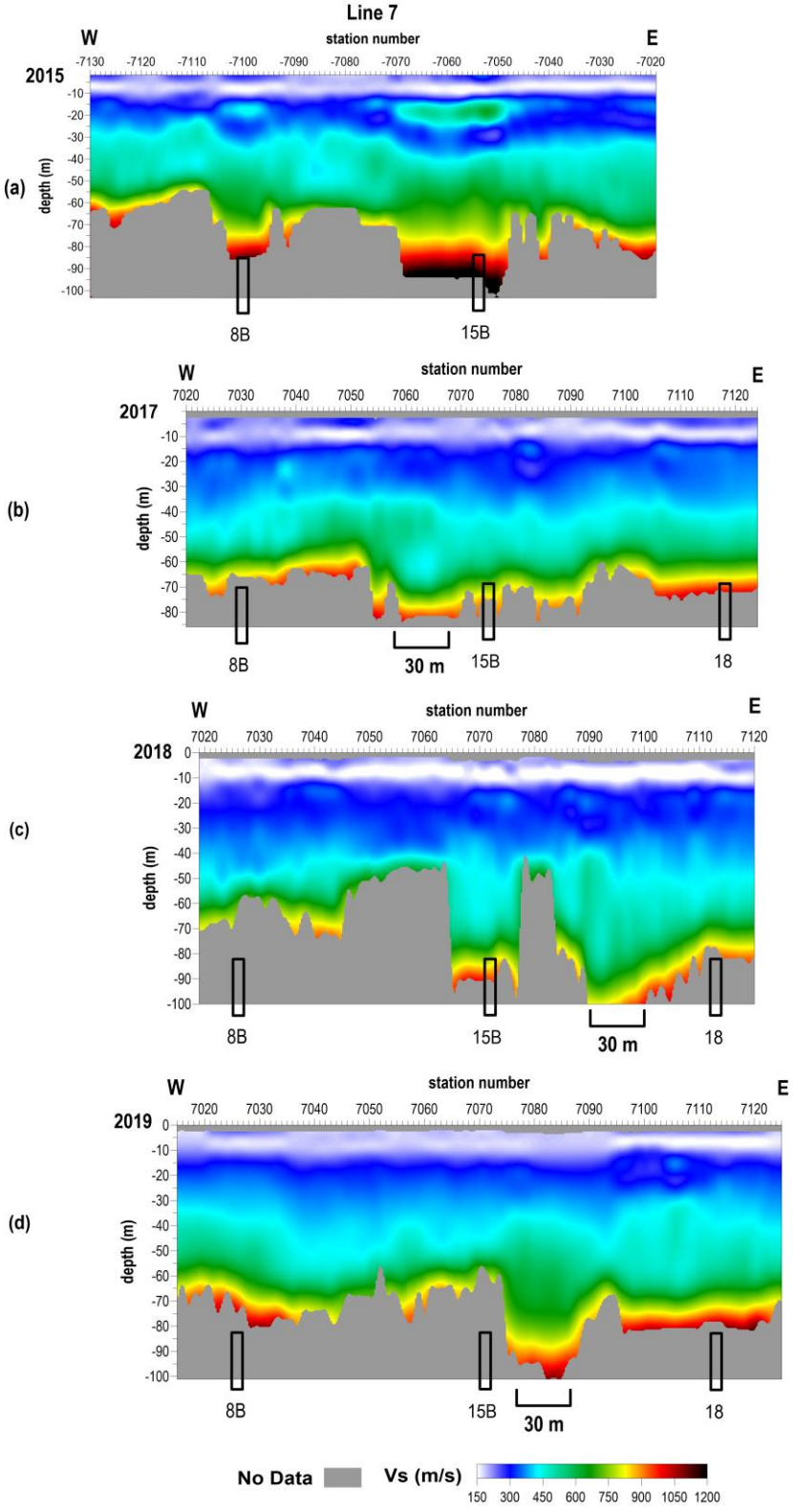

A1. Shear-wave velocity profiles from line 7 from (a) March 2015, (b) November 2017, (c) December 2018, and (d) the December 2019 investigation with approximate well locations.

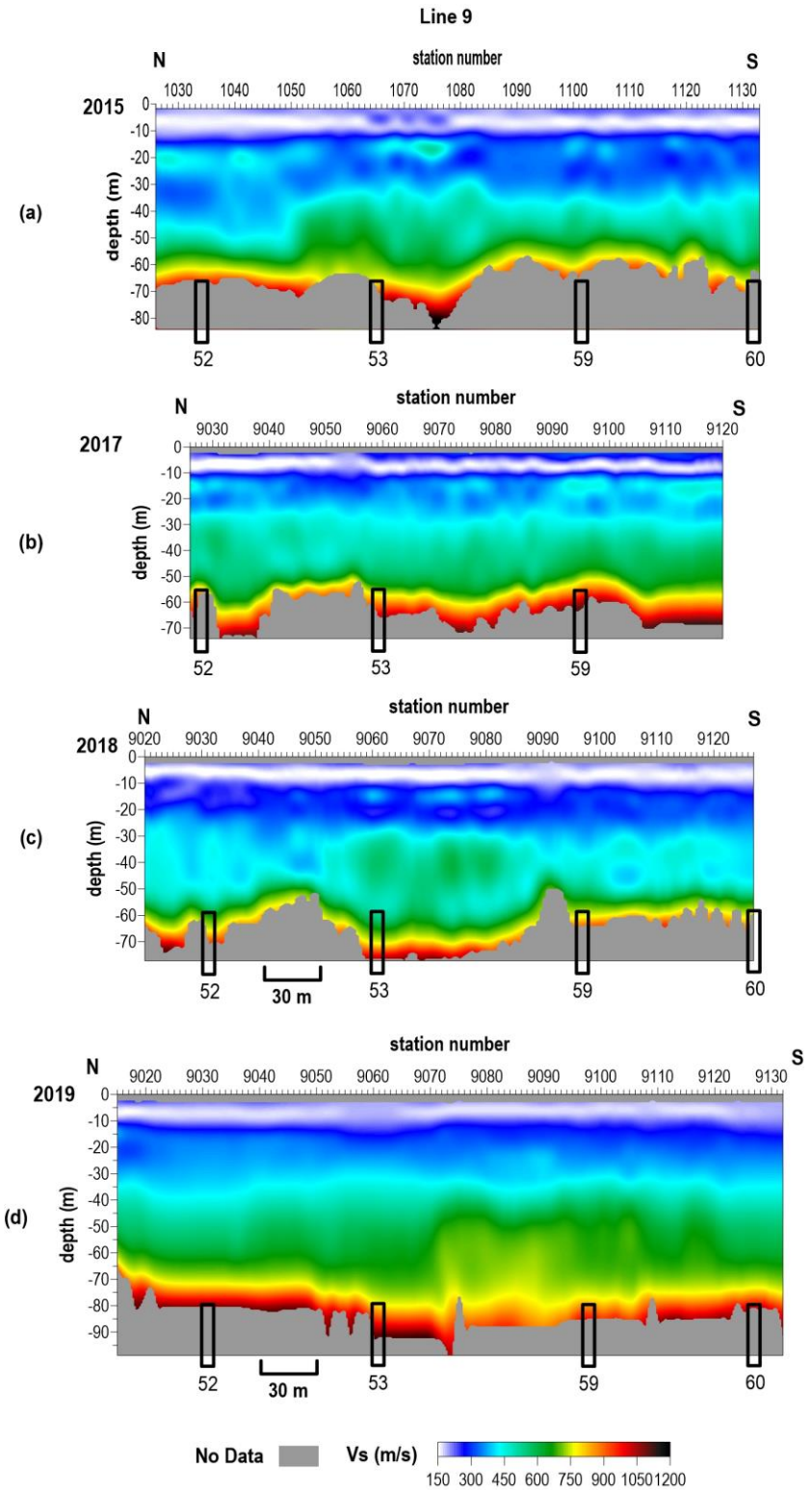

A2. Shear-wave velocity profiles from line 9 from (a) March 2015, (b) November 2017, (c) October 2018, and (d) the December 2019 investigation with approximate well locations.

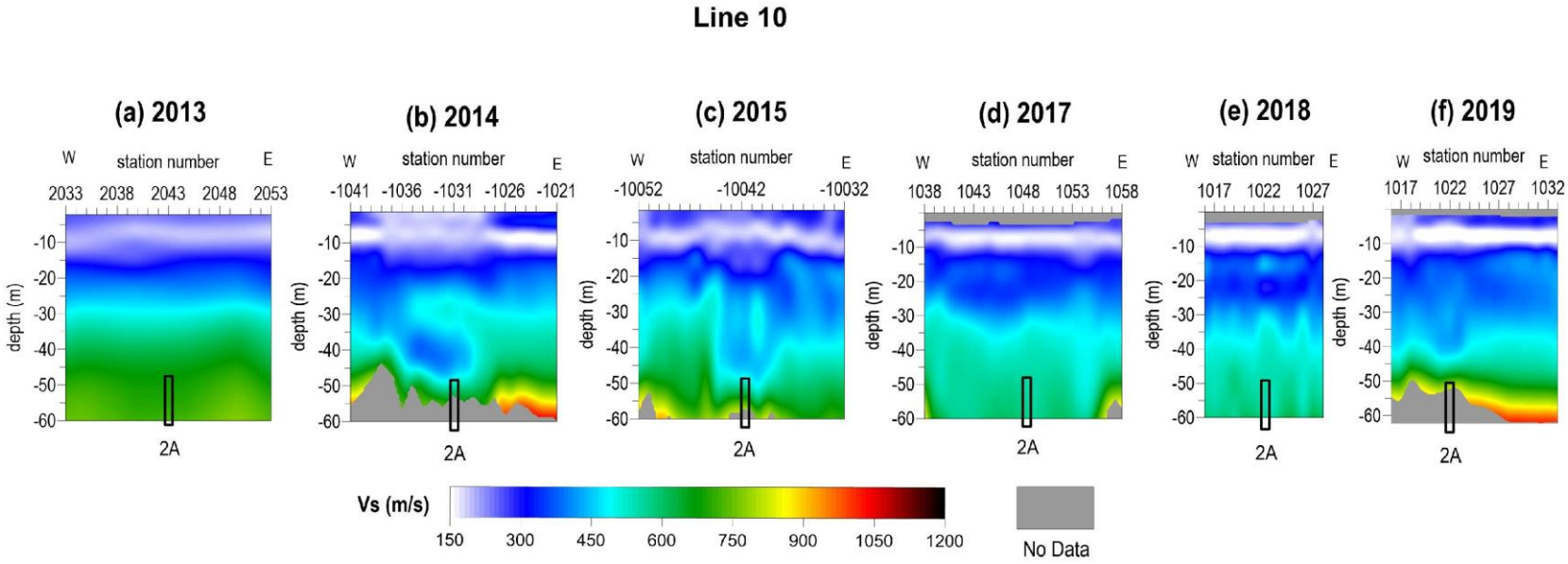

A3. Shear-wave velocity profiles from line 10 from (a) March 2013, (b) November 2014, (c) Mary 2015, (d) November 2017, (e) October 2018, and (f) the December 2019 investigation with approximate well locations.

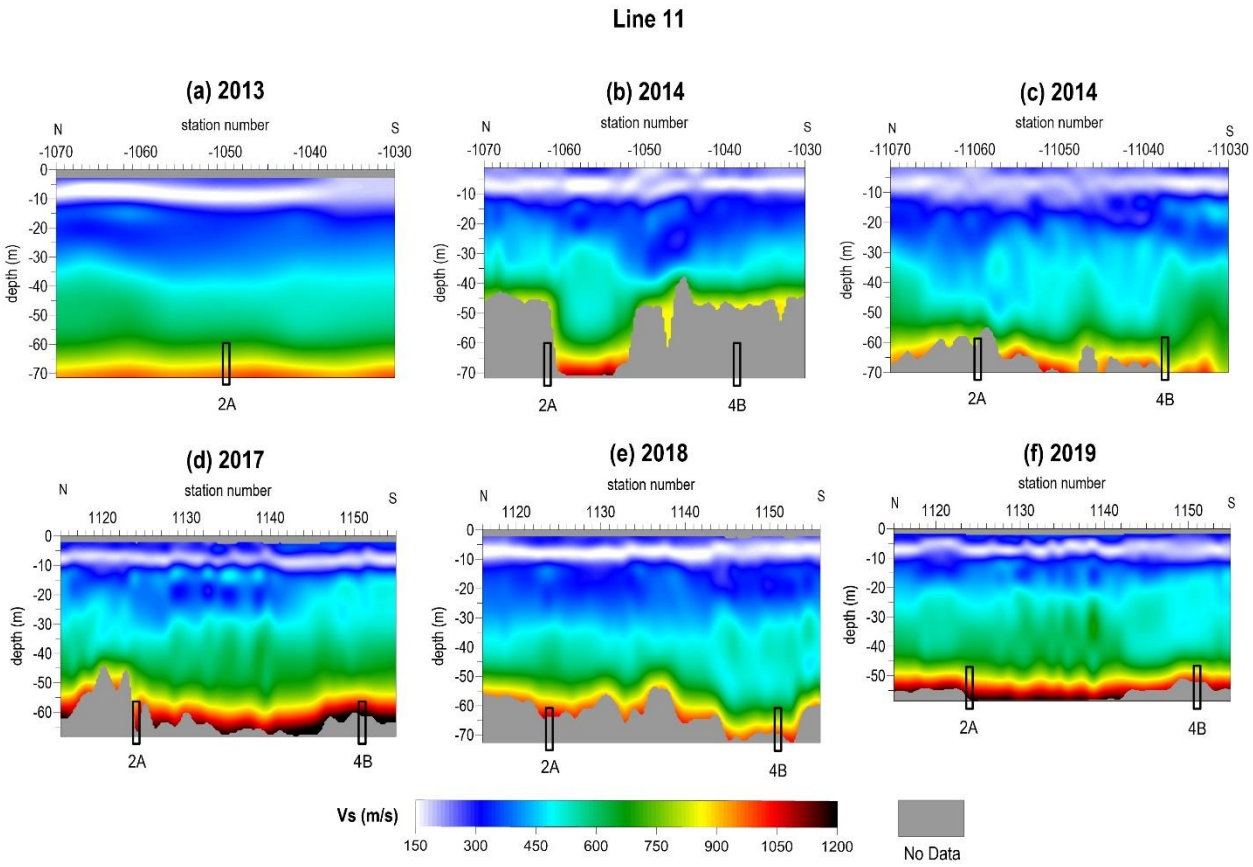

A4. Shear-wave velocity profiles from line 11 from (a) March 2013, (b) November 2014, (c) May 2015, (d) November 2017, (e) October 2018, and (f) the December 2019 investigation with approximate well locations.

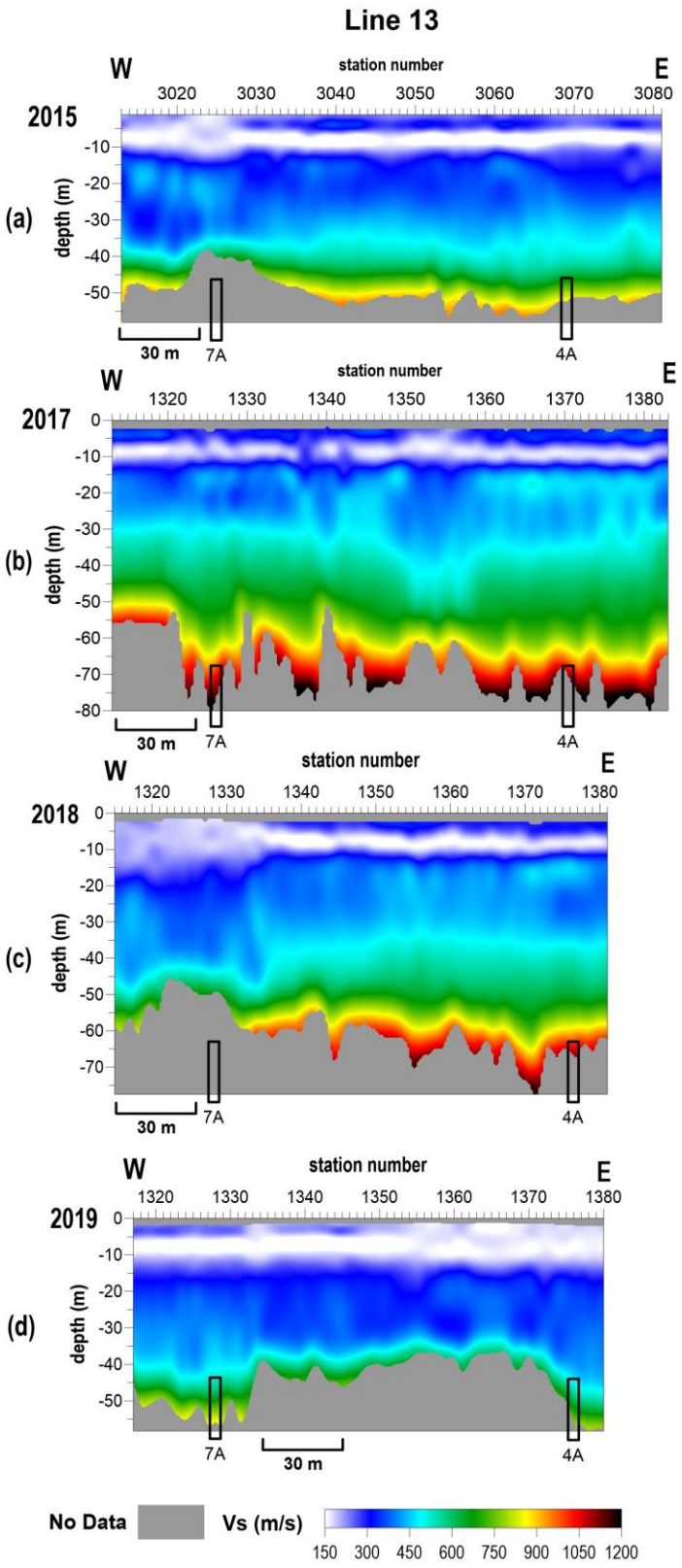

A5. Shear-wave velocity profiles from line 13 from (a) March 2015, (b) November 2017, (c) December 2018, and (d) the December 2019 investigation with approximate well locations.